

The absorption non-symmetric ion-atom processes in the helium-rich white dwarf atmospheres

Lj. M. Ignjatović^{1,2} *, A. A. Mihajlov^{1,2}, V. A. Srećković^{1,2}
and M. S. Dimitrijević^{2,3,4,5}

¹University of Belgrade, Institute of Physics, P. O. Box 57, 11001 Belgrade, Serbia

²Isaac Newton Institute of Chile, Yugoslavia Branch, Volgina 7, 11060 Belgrade, Serbia

³Astronomical Observatory, Volgina 7, 11160 Belgrade 74, Serbia

⁴IHIS-Technoexperts, Bežanijska 23, 11080 Zemun, Serbia

⁵Observatoire de Paris, 92195 Meudon Cedex, France

ABSTRACT

In this work the processes of absorption charge-exchange and photo-association in $\text{He}+\text{H}^+$ collisions together with the process of ion HeH^+ photo-dissociation are considered as factors of influence on the opacity of the atmospheres of helium-rich white dwarfs in the far UV and EUV region. It is shown that they should be taken into account even in the cases of the atmospheres of white dwarfs with $\text{H}:\text{He}=10^{-5}$. Then, it is established that in the cases of white dwarfs with $\text{H}:\text{He} \gtrsim 10^{-4}$, particularly when $\text{H}:\text{He} \approx 10^{-3}$, these processes have to be included *ab initio* in the corresponding models of their atmospheres, since in the far UV and EUV region they become dominant with respect to the known symmetric ion-atom absorption processes.

Key words: (stars:) white dwarfs – stars: atmospheres – radiation mechanisms: general – radiative transfer – atomic processes – molecular processes

1 INTRODUCTION

It has been shown recently in Mihajlov et al. (2013), that in order to consider the contribution of the absorption processes connected with binary ion-atom systems to the opacity of the solar photosphere it is not enough to take into account only the processes of absorption charge exchange in $(\text{H} + \text{H}^+)$ -collisions and the molecular ion H_2^+ photo-dissociation. These processes were studied in Mihajlov & Dimitrijević (1986) and Mihajlov et al. (1993, 1994b, 2007), and are already included in one of the solar photosphere models (Fontenla et al. 2009). It has been established that in the very important far UV and EUV spectral regions they have to be considered together with the processes of the absorption charge exchange and photo-association in non-symmetric $(\text{H} + \text{X}^+)$ -collisions and molecular ion HX^+ photo-dissociation, where X is one of metal atoms. Namely, it has been proved that only in such case the total efficiency of the ion-atom absorption processes in the mentioned spectral regions approaches the efficiency of the relevant concurrent processes in the whole solar photosphere.

These results suggest that it is useful to consider again

the situation of ion-atom absorption processes in the atmospheres of helium-rich white dwarfs. Let us remind that in the previous papers (Mihajlov & Dimitrijević 1992; Mihajlov et al. 1994a; Stancil 1994; Mihajlov et al. 1995; Ignjatović et al. 2009), dedicated to certain DB white dwarf atmospheres, the processes of molecular ion He_2^+ photo-dissociation were studied:

$$\varepsilon_\lambda + \text{He}_2^+ \longrightarrow \text{He} + \text{He}^+, \quad (1)$$

and absorption charge exchange in $(\text{He} + \text{He}^+)$ -collisions:

$$\varepsilon_\lambda + \text{He}^+ + \text{He} \longrightarrow \text{He} + \text{He}^+ \quad (2)$$

where ε_λ is the energy of a photon with wavelength λ , $\text{He} = \text{He}(1s^2)$, $\text{He}^+ = \text{He}^+(1s)$ and $\text{He}_2^+ = \text{He}_2^+(1^2\Sigma_u^+)$. The significance of these symmetric ion-atom absorption processes for the atmospheres of the considered DB white dwarfs was established in Mihajlov et al. (1994a, 1995) and Ignjatović et al. (2009) by a direct comparison of their efficiencies with the main concurrent process of inverse "bremsstrahlung" in (free electron + He)-collisions, i.e.

$$\varepsilon_\lambda + e + \text{He} \longrightarrow e' + \text{He}, \quad (3)$$

where e and e' denote a free electron in the initial and final energetic states respectively. For that purpose the data from the corresponding DB white-dwarf atmosphere models

* E-mail: ljuba@ipb.ac.rs

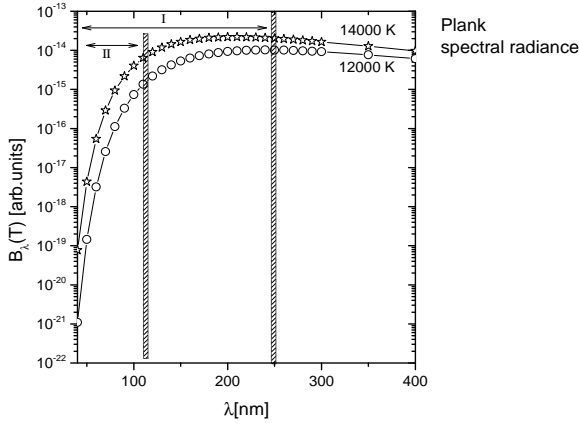
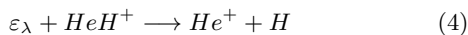


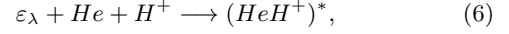
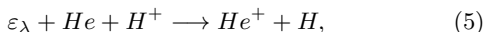
Figure 1. Plank curve for $T_{eff} = 12000$ K and $T_{eff} = 14000$ K. "I" and "II" denote the regions $50.44 \text{ nm} \leq \lambda \lesssim 250 \text{ nm}$ and $50.44 \text{ nm} \leq \lambda \lesssim 120 \text{ nm}$ respectively.

(Koester 1980) have been used. It was established that the processes (1) and (2) significantly influence the opacity of the considered DB white dwarf atmospheres, with an effective temperature $T_{eff} \geq 12000$ K, which fully justifies their inclusion in one of the models of such atmospheres (Bergeron et al. 1995). However, the same comparison demonstrated also that the dominant role in those atmospheres generally still belongs to the concurrent absorption process (3), while the processes (1) and (2) can be treated as dominant (with respect to this concurrent process) only in some layers of that atmospheres, and only within the part $50 \text{ nm} < \lambda < 250 \text{ nm}$ of the far UV and EUV region. In Fig. 1, where Plank's curves for $T_{eff} = 12000$ K and 14000 K are shown, this part is denoted by "I". Its boundary (from the short-wavelength side) is determined by the value of wavelength $\lambda_{He} \approx 50.44 \text{ nm}$, which corresponds to the threshold of the atom He photo-ionization. Hence it follows that in the case of helium-rich white dwarf atmospheres it would certainly be useful to include into consideration some new ion-atom absorption processes, which is principally allowed in accordance with the composition of such atmospheres (Bues 1970).

Let us note in this context that in the case of white dwarf atmospheres with dominant helium component, among all possible symmetric ion-atom absorption processes which are allowed by their composition (Bues 1970), only the processes (1) and (2) have to be taken into account. This means that in this case we can find new relevant absorption processes only among the processes connected with non-symmetric ion-atom systems, particularly such systems which could provide efficiency in the same part "I" of the far UV and EUV region. Here we will examine the significance of non-symmetric ion-atom absorption processes with participation of the hydrogen component. We mean the processes of molecular ion HeH^+ photo-dissociation



and the processes of absorption charge exchange and photo-association in the $(\text{He} + \text{H}^+)$ -collisions, namely

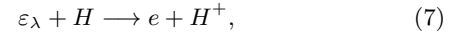


where $\text{H} = \text{H}(1s)$, $\text{He} = \text{He}(1s^2)$, $\text{He}^+ = \text{He}^+(1s)$, and HeH^+ and $(\text{HeH}^+)^*$ denote the molecular ion in the ground and the first excited electronic states which are adiabatically correlated with the states of the systems $\text{He} + \text{H}^+$ and $\text{He}^+ + \text{H}$ respectively at the infinite internuclear distance. Already in Mihajlov et al. (2013) it was noted that these processes, whose significance was practically neglected for the solar photosphere, could be rather important in the case of helium-rich white dwarf atmospheres. This assumption was worthy of attention, particularly due to the fact that characteristics of the considered non-symmetric molecular ions (see Fig. 2) provide manifestations of the processes (4) - (6) just in the part "I" of the far UV and EUV region.

In connection with this fact, let us remind that the part "I" is rather important for such values of T_{eff} . Namely, let λ_{max} be the positions of the maxima of the spectral intensities characterizing the electromagnetic (EM) emission of the considered atmospheres, which are determined from the well-known Wien's law: $\lambda_{max} \cdot T_{eff} = 2.898 \cdot 10^6 \text{ nm} \cdot \text{K}$. We then have it that for the considered DB white dwarfs $\lambda_{max} < 250 \text{ nm}$, so that the mentioned maxima lie just within the region "I".

It was just because of the above mentioned that this investigation was undertaken. The main aim was to study when the non-symmetric absorption processes (4) - (6) can significantly influence the opacity of helium-rich white dwarf atmospheres in the part "I" of the UV and VUV spectral region, and to show that the processes (4) - (6) deserve to be included *ab initio* in the corresponding white dwarf atmosphere models. Therefore the relevant spectral characteristics of the processes (4) - (6) are determined here for the atmospheres of different helium-rich white dwarfs with $T_{eff} = 12000$ K and 14000 K, $\log g = 8$ and 7 , and for the values of the ratio H:He from 10^{-5} to 10^{-3} . The necessary expressions for these spectral characteristics are given in Section 2. Then, with their help, in the Section 3 the values are calculated of the parameters characterizing the relative efficiency of the non-symmetric processes (4) - (6) with respect to the efficiency of all ion-atom processes, as well as with respect to the electron-atom process (3), which comprise the main direct results of this work.

Let us note that already in (Ignjatović et al. 2009), beside the electron-atom processes (3) the process of photoionization of hydrogen atoms, was also considered, namely



where $\text{H} = \text{H}(1s)$. It was treated as a concurrent process, potentially necessary in the region $\lambda < \lambda_H$ where $\lambda_H \approx 911 \text{ \AA}$ corresponds to the threshold of atom H photoionization. However, in (Bergeron 2013) it was brought to attention that the importance of this absorption channel was significantly underestimated. That is why in this work the process (7) was again included into the consideration and carefully examined.

One can see that in this work we take into account only such non-symmetric ion-atom absorption processes where, apart from the dominant helium component of the considered atmospheres, only the hydrogen component participates, although they contain also a lot of metal components (Bues 1970). This is due to the fact that the existing at-

mosphere models do not provide the necessary data (about the relevant metals' abundances) which would be needed for the present calculations. However, we consider that a demonstration of the fact that for the considered atmospheres the processes (4) - (6), where one of their "minor" components participates, are rather significant, is a sufficient reason for treating the non-symmetric ion-atom absorption processes in general as potentially significant for those atmospheres.

2 THE THEORETICAL REMARKS: THE RELEVANT SPECTRAL CHARACTERISTICS

2.1 The non-symmetric ion-atom processes

As the relevant characteristics of the processes (4), (5) and (6) we will use the corresponding spectral absorption coefficients. They are defined as functions of $\log \tau$, where τ is Rosseland optical depth of the part of the examined atmosphere above the considered layer for the wavelength λ . They are denoted here as $\kappa_{nsim}^{(bf)}(\lambda; \log \tau)$, $\kappa_{nsim}^{(ff)}(\lambda; \log \tau)$ and $\kappa_{nsim}^{(fb)}(\lambda; \log \tau)$, in accordance with the fact that the mentioned processes can be treated as bound-free, free-free and free-bound respectively. These coefficients are determined here within the corresponding atmosphere models, by means of the local temperature and the densities of He atoms and H^+ ions, and used in a similar form, namely

$$\kappa_{nsim}^{(bf,ff,fb)}(\lambda; \log \tau) = K_{nsim}^{(bf,ff,fb)}(\lambda; T) N_{He} N_{H^+}, \quad (8)$$

where $T \equiv T(\log \tau)$, $N_{He} \equiv N_{He}(\log \tau)$ and $N_{H^+} \equiv N_{H^+}(\log \tau)$. Of course, it is understood that the photo-dissociation rate coefficient $K_{nsim}^{(bf)}(\lambda; T)$ is given by the known relations

$$K_{nsim;X}^{(bf)}(\lambda; T) = \sigma_{HeH^+}^{(phd)}(\lambda, T) \cdot \chi^{-1}(T; HeH^+), \quad (9)$$

$$\chi(T; HeH^+) = \left[\frac{N_{He} \cdot N_{H^+}}{N_{HeH^+}} \right], \quad (10)$$

where $\sigma_{HeH^+}^{(phd)}(\lambda, T)$ is the mean thermal cross-section for the molecular ion HeH^+ photo-dissociation, N_{HeH^+} denotes the local density of these molecular ions, and $\chi(T; HeH^+)$ is determined under condition of local thermodynamical equilibrium (LTE) with given T , N_{He} and N_{H^+} . Let us note that these expressions contain no correction factors which take into account the influence of stimulated emission, since within the actual range of ε_λ/kT ratio for the considered cases the changes due to these factors will be of the order of magnitude of $10^{-3}\%$.

Finally, the total efficiency of the non-symmetric processes (4), (5) and (6) is characterized here by the spectral absorption coefficient $\kappa_{nsim}(\lambda; \log \tau)$ given by the relations

$$\kappa_{nsim}(\lambda; \log \tau) = K_{nsim}(\lambda; T) N_{He} N_{H^+}, \quad (11)$$

$$K_{nsim}(\lambda; T) = K_{nsim}^{(bf)}(\lambda; T) + K_{nsim}^{(ff)}(\lambda; T) + K_{nsim}^{(fb)}(\lambda; T), \quad (12)$$

where the rate coefficients $K_{nsim}^{(bf,ff,fb)}(\lambda, T)$ are determined by means of the necessary characteristics of the considered molecular ion, in a way which was described in detail in Mihajlov et al. (2013).

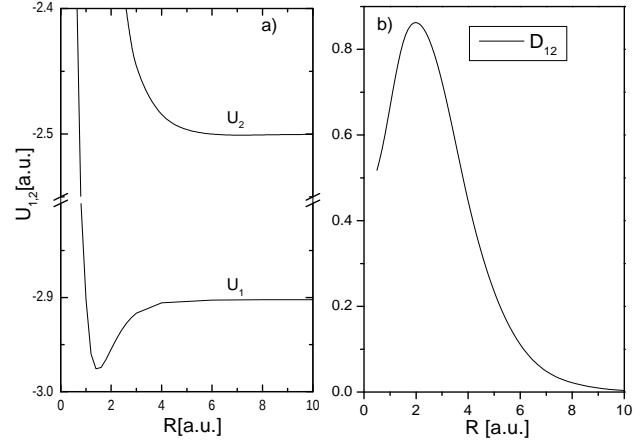


Figure 2. The potential curves $U_1(R)$ and $U_2(R)$ for the ground and the first excited electronic states of the molecular ion HeH^+ and the corresponding dipole matrix element $D_{12}(R)$, where R is the internuclear distance.

The mentioned characteristics, i.e. the adiabatic potential curves of the molecular ion in the ground state (HeH^+) and the first excited electronic state ($(HeH^+)^*$), as well as the corresponding dipole matrix element (which were not shown in Mihajlov et al. (2013)) are presented here in Fig.2 as functions of the internuclear distance R . This figure also shows in a schematic way the bound-free (bf), free-free (ff) and free-bound (fb) transitions between the energy states of the considered ion-atom system which correspond to the processes (4), (5) and (6). The potential curves are denoted in Fig. 2 by $U_1(R)$ and $U_2(R)$, and dipole matrix element - by $D_{12}(R)$. Their values as functions of R are determined here by fitting the corresponding data from Green et al. (1974b) and Green et al. (1974a).

Let us note that these data have a shortcoming: they are not sufficiently complete and do not guarantee that different ways of fitting give close values of $U_1(R)$, $U_2(R)$ and $D_{12}(R)$. It is possible that this shortcoming causes the observed differences between our values of the partial cross-section for photo-dissociation of the ion HeH^+ from its ground rovibrational state and the values presented in Dumitriu & Saenz (2009), where they were calculated by means of the same data. However, here we used just the data from Green et al. (1974b) and Green et al. (1974a) since as yet only these papers give at least some data about both the necessary potential curves (of the ion HeH^+) and the corresponding matrix element. Also, we keep in mind that development of numerical procedures which would be suitable for improvement of the data presented in Green et al. (1974b) and Green et al. (1974a) far exceeds the aim of this work. Apart from that, we consider that the deviations of the potential curves $U_1(R)$ and $U_2(R)$ from the hypothetical exact ones do not cause any large errors in the obtained results and consequently cannot strongly influence the final conclusions.

Since all processes (4) - (6) are connected with the transition between the ground and the first excited electronic states of the strongly non-symmetric ion-atom system (HeH^+ or $He + H^+$) we have it that the range of values of the splitting term ($U_{12}(R) \equiv U_2(R) - U_1(R)$) well char-

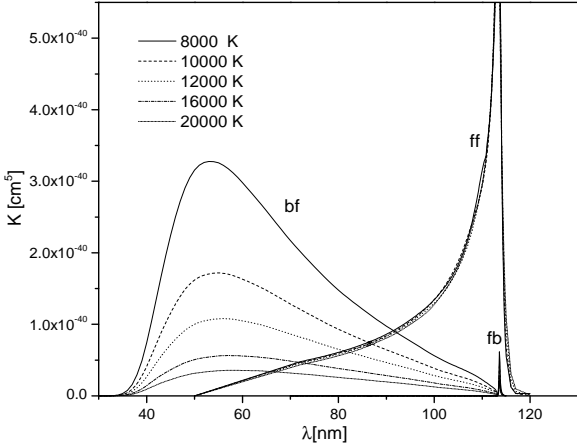


Figure 3. The behavior of the bound-free (bf), free-free (ff) and free-bound (fb) spectral rate coefficients $K_{HeH^+}^{(bf,ff,fb)}(\lambda; T)$ for the molecular ion HeH^+ .

acterizes the range of photon energies which is relevant for those processes. It is just due to this fact that we could state above that the processes (4) - (6) have to be manifested in the part "I" of the far UV and EUV spectral region (see Fig. 1).

Although the behavior of the rate coefficients $K_{nsim}^{(bf,ff,fb)}(\lambda, T)$ was already discussed in Mihajlov et al. (2013), it is also illustrated here by Fig. 3 since the range of temperatures characterizing the solar photosphere is not relevant in our case. These figures give a possibility to estimate that the processes (4) - (6) can be significant in the spectral region denoted in Fig. 1 by "II".

2.2 The symmetric ion-atom, electron-atom and hydrogen photo-ionization processes

For the sake of the following considerations we have to introduce the spectral coefficients $\kappa_{sim}(\lambda; \log \tau)$, $\kappa_{e-He}(\lambda; \log \tau)$ and $\kappa_{phi}(\lambda; \log \tau)$ which characterize the efficiencies of the symmetric ion-atom absorption processes (1) and (2) together, the electron-atom processes (3) and hydrogen photoionization process (7) respectively. As in Ignjatović et al. (2009) we can take these coefficients in the known form:

$$\kappa_{sim}(\lambda; \log \tau) = K_{sim}(\lambda, T) \cdot N_{He} \cdot N_{He^+}, \quad (13)$$

$$\kappa_{e-He}(\lambda; \log \tau) = K_{e-He}(\lambda, T) \cdot N_{He} \cdot N_e, \quad (14)$$

$$\kappa_{phi}(\lambda; \log \tau) = \sigma_{phi}(\lambda; H) \cdot N_H, \quad (15)$$

where N_{He^+} , N_e and N_H are the local densities of ions He^+ , free electrons and atoms H, $K_{sim}(\lambda, T)$ and $K_{e-He}(\lambda, T)$ - adequately defined spectral rate coefficients, and $\sigma_{phi}(\lambda; H)$ - spectral cross-section for atom H photoionization. The absorption coefficient $K_{sim}(\lambda, T)$ is determined in the way which is described in detail in Ignjatović et al. (2009), and $K_{e-He}(\lambda, T)$ - by means of the data from Somerville (1965), and $\sigma_{phi}(\lambda; H)$ is taken from (Bethe & Salpeter 1957).

Here we take into account the fact that all the values of the rate coefficients $K_{sim}(\lambda, T)$ and $K_{e-He}(\lambda, T)$ which are

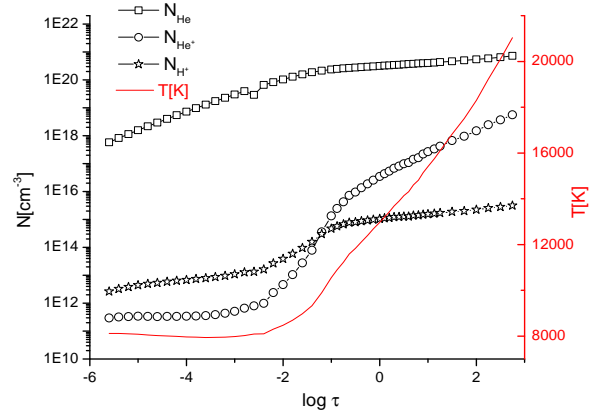


Figure 4. The local densities N_{He} , N_{He^+} and N_{H^+} and the temperature T as functions of $\log \tau$, where τ is Rosseland optical depth, according to the model of the DB white dwarf atmosphere from (Koester 1980) for: $T_{eff}=12000$ K, $\log g = 8$ and $H:He=10^{-5}$.

needed for our calculations have already been determined in Ignjatović et al. (2009), and that the photo-ionization cross-section $\sigma_{phi}(\lambda; H)$ is given by a known analytical expression. Therefore in the further text we will simply treat these characteristics and, consequently, the spectral absorption coefficients $\kappa_{sim}(\lambda, \log \tau)$, $\kappa_{e-He}(\lambda, \log \tau)$ and $\kappa_{phi}(\lambda; \log \tau)$ as known quantities.

3 RESULTS AND DISCUSSION

3.1 DB white dwarfs

As it is well known, the above defined spectral absorption coefficients depend on the wavelength, local temperature, and local particle densities, based on the corresponding models of helium-rich white dwarf atmospheres characterized by certain values of T_{eff} , $\log g$ and the ratio of the hydrogen and helium species (H:He). Here we will start from DB white dwarf atmospheres with $T_{eff} = 12000$ K and 14000 K, $\log g = 8$ and 7 and $H:He = 10^{-5}$. For their description we will use the equilibrium models which are presented in Koester (1980). As in Mihajlov et al. (1994a, 1995), and Ignjatović et al. (2009), it is due to the fact that, although newer atmosphere models for helium-rich white dwarfs now exist (see e.g. the review article of Koester (2010)), only the models from Koester (1980) contain in a tabular form all the relevant data which are needed for our calculations.

The behavior of the densities of free electrons and ions He^+ and H^+ in the atmosphere of a DB white dwarf with $T_{eff} = 12000$ K and $\log g = 8$ is illustrated by Fig. 4, which shows that the processes (4) - (6) could be of interest already in the case $H:He = 10^{-5}$. Namely, this figure suggests that for $T_{eff} \lesssim 14000$ K, the ion H^+ density is even larger than that of He^+ in significant parts of DB white dwarfs' atmospheres ($\log \tau < -1$).

In accordance with the aim of this work we have to estimate first the relative efficiency of the non-symmetric processes (4) - (6) with respect to the total efficiency of all

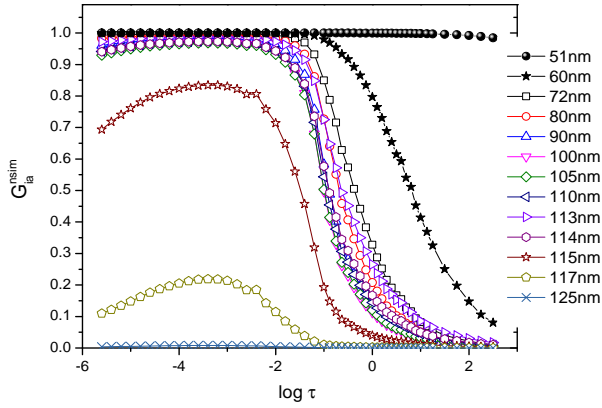


Figure 5. The behavior of the quantity $G_{ia}^{nsim} = \kappa_{nsim}/\kappa_{ia}$, see Eq. (17), for DB white dwarf atmosphere with $T_{eff}=12000$ K, $\log g = 8$ and $H/He=10^{-5}$.

the above mentioned ion-atom absorption processes, which is characterized by the spectral absorption coefficient

$$\kappa_{ia}(\lambda; \log \tau) = \kappa_{nsim}(\lambda; \log \tau) + \kappa_{sim}(\lambda; \log \tau), \quad (16)$$

For that purpose we use the quantity

$$G_{ia}^{(nsim)}(\lambda; \log \tau) = \frac{\kappa_{nsim}(\lambda; \log \tau)}{\kappa_{ia}(\lambda; \log \tau)}. \quad (17)$$

One can see that the definition of this quantity guarantees the validity of the relations $0 < G_{ia}^{(nsim)}(\lambda; \log \tau) < 1$ for any λ and $\log \tau$. It is important since other possible quantities, i.e. $\kappa_{ia}(\lambda; \log \tau)/\kappa_{sim}(\lambda; \log \tau)$ and $\kappa_{nsim}(\lambda; \log \tau)/\kappa_{sim}(\lambda; \log \tau)$, could not be practically presented in the corresponding figure.

The behavior of the quantity $G_{ia}^{(nsim)}(\lambda; \log \tau)$ for a DB white dwarf atmosphere with $T_{eff} = 12000$ K, $\log g = 8$ and $H:He = 10^{-5}$ is illustrated by Fig. 5. This figure shows that the non-symmetric processes (4) - (6) are dominant within a significant part of the considered atmosphere ($-5.6 \leq \log \tau \lesssim -0.75$), which corresponds to the part in Fig. 4 where $N_{H^+} > N_{He^+}$.

In order to establish how the inclusion of the non-symmetric processes (4) - (6) into the consideration influences the relative efficiency of the ion-atom absorption processes with respect to the efficiency of the concurrent electron-atom process (3), we calculated the quantities

$$\begin{aligned} F_{e-He}^{(sim)}(\lambda; \log \tau) &= \frac{\kappa_{sim}(\lambda; \log \tau)}{\kappa_{e-He}(\lambda; \log \tau)}, \\ F_{e-He}^{(ia)}(\lambda; \log \tau) &= \frac{\kappa_{ia}(\lambda; \log \tau)}{\kappa_{e-He}(\lambda; \log \tau)}. \end{aligned} \quad (18)$$

Comparison of these two quantities gives a possibility to estimate the change of the mentioned relative efficiency. The behavior of these quantities in the case of the considered DB white dwarf atmosphere ($T_{eff} = 12000$ K, $\log g = 8$, $H:He = 10^{-5}$) is shown in Fig. 6. From this figure one can see that:

- the inclusion of the ion-atom non-symmetric absorption processes causes a very significant increase in the relative efficiency of the ion-atom absorption processes in just that

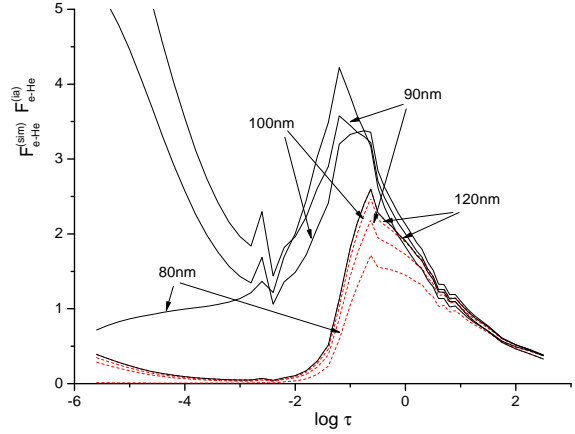


Figure 6. The behavior of the quantities $F_{e-He}^{(sim)}(\lambda; \log \tau) = \kappa_{sim}/\kappa_{ea}$ (red line-dashed) and $F_{e-He}^{(ia)}(\lambda; \log \tau) = \kappa_{ia}/\kappa_{ea}$ (black line-full), see Eq. (18), for DB white dwarf atmosphere with $T_{eff}=12000$ K, $\log g = 8$ and $H/He=10^{-5}$.

region $\log \tau < 0.75$, i.e. where the symmetric processes can be practically neglected.

Then, we established the fact that the behavior of the quantities $G_{ia}^{(nsim)}(\lambda; \log \tau)$, $F_{e-He}^{(sim)}(\lambda; \log \tau)$ and $F_{e-He}^{(ia)}(\lambda; \log \tau)$ is also similar in the cases of DB white dwarf atmospheres with the same value of $H:He$, but with $T_{eff} = 14000$ K and $\log g = 8$, and $T_{eff} = 12000$ K and $\log g = 7$. Based on the above mentioned, it can be concluded that the non-symmetric processes (4) - (6) have a visible significance for the atmospheres of the considered DB white dwarfs with $H:He = 10^{-5}$ and should be included in their models.

It is necessary to draw attention to the fact that this conclusion refers to a spectral region $\lambda > \lambda_H$ where the hydrogen photo-ionization process (7) is impossible. In order to estimate the partial efficiencies of the mentioned processes in the case of the considered DB white dwarf in the whole region $\lambda > \lambda_{He}$ the corresponding plots of all discussed absorption processes for $\log \tau = 0$ are presented in Fig. 7. One can see that in the region $\lambda_{He} < \lambda < \lambda_H$ the process (7) alone gives the dominant contribution to the opacity of the considered atmosphere. Here it was established that in the considered case this dominance exists for any $\log \tau < 0$.

However, the main results of the research of DB white dwarf atmospheres is the establishment of the fact that:

- the inclusion of the non-symmetric processes causes an increase of the total efficiency of ion-atom absorption processes in the region $0.75 < \log \tau < 2$, where the symmetric processes (1) and (2) are dominant, which is not negligible but rather reaches several percent.

3.2 Other helium rich white dwarfs.

The mentioned result is important for our further research since it leads to an expectation that the significance of the considered non-symmetric ion-atom absorption processes could be much greater in the cases of the atmospheres of some other helium-rich white dwarfs. We mean the atmo-

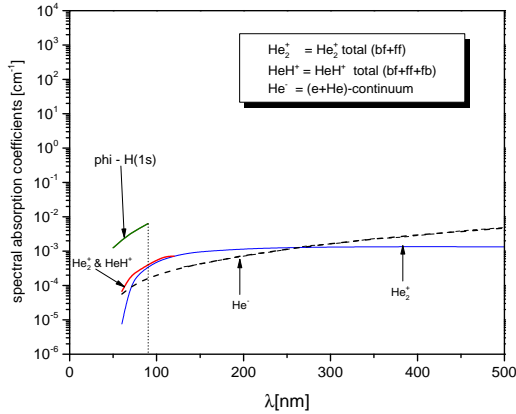


Figure 7. The plots of all considered absorption processes for $\log \tau = 0$ in the case of a DB white dwarf with $T_{eff}=12000$ K, $\log g = 8$ and $H:He=10^{-5}$.

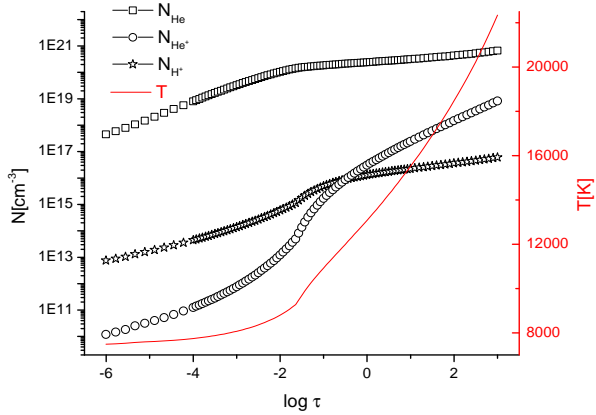


Figure 8. The local densities N_{He} , N_{He^+} and N_{H^+} , and the temperature T as functions of $\log \tau$, where τ is Rosseland optical depth, according to the developed model of helium-rich white dwarf atmosphere for: $T_{eff}=12000$ K, $\log g = 8$ and $H:He=10^{-4}$.

spheres with the same or similar T_{eff} and $\log g$, but with the values of the ratio $H:He$ which are larger by one or even two orders of magnitude.

In this context let us note that in [Wegner & Koester \(1985\)](#) some DC white dwarfs with $T_{eff} \approx 12500$ K, $\log g = 8$ and $H:He = 2 \cdot 10^{-4}$ are described. Then, in [Dufour et al. \(2006\)](#) some weakly magnetic DZ white dwarfs with $\log g = 8$, $T_{eff} \approx 7000$ K and $H:He \approx 10^{-3}$ are discussed. Finally, we will remind also that in [Dufour et al. \(2007\)](#) some DZ white dwarfs with $\log g \approx 8$, $T_{eff} > 12000$ K and $H:He = 10^{-4}$ and 10^{-3} are mentioned, as well as a number of other DZ white dwarfs with $\log g \approx 8$, the values of T_{eff} from about 6500 K to about 10000 K, and the values of $H:He$ from about $10^{-3.2}$ to about $10^{-4.4}$. Just from the above mentioned result it follows that the contribution of the non-symmetric processes (4) - (6) to the opacity of such atmospheres should be very significant. Namely, although the

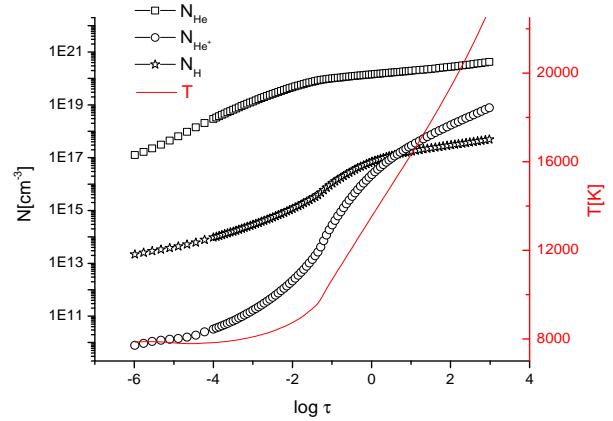


Figure 9. Same as in Fig. 8, but for $H:He=10^{-3}$.

ion H^+ density cannot increase proportionally to the ratio $H:He$, an increase of this ratio of 10 or 100 times, has to cause an increase of N_{H^+} of at least several times. So, the mentioned increase of several percent in region $-1 < \log \tau \leq 2$ in the case of DB white dwarf atmospheres has to become an increase of several tens of percent in the cases of the helium-rich white dwarfs with $10^{-4} \lesssim H:He \lesssim 10^{-3}$.

In order to check our expectations we performed calculations of the quantity $G_{ia}^{(nsim)}$, as well as of the quantities $(\lambda; \log \tau)$, $F_{e-He}^{(sim)}(\lambda; \log \tau)$ and $F_{e-He}^{(ia)}(\lambda; \log \tau)$, simulating the behavior of T , N_{He} , N_{H^+} and other particle densities, in helium-rich white dwarf atmospheres with $T_{eff} = 12000$ K, $\log g = 8$ and $H:He > 10^{-5}$. All the needed calculations have been performed on the basis of the models taken from [Koester \(2013\)](#). In Figs. 8 and 9 the corresponding densities N_{H^+} , N_{He^+} and N_e are shown as functions of $\log \tau$ for $H:He = 10^{-4}$ and 10^{-3} respectively. One can see, by comparing these figures and Fig. 4, that the considered increase of the ratio $H:He$ indeed causes a very significant increase of N_{H^+} .

The behavior of $G_{ia}^{(nsim)}(\lambda; \log \tau)$ in the considered spectral region (denoted by "II" in Fig. 1) is shown in Fig. 10 for $H:He = 10^{-4}$ and in Fig. 11 for $H:He=10^{-3}$. By comparing Fig.10 and Fig.5 it can be seen that for $51 \text{ nm} \leq \lambda \leq 125 \text{ nm}$ an increase of the ratio $H:He$ from 10^{-5} to 10^{-4} causes a visible increase of participation of the considered non-symmetric processes (with respect to the total ion-atom spectral absorption coefficient) for $\log \tau > -1$ and a significant increase for $\log \tau > 0$. Then, by comparing Fig. 5 and Fig. 11 it is seen that an increase of the ratio $H:He$ from 10^{-5} to 10^{-3} causes yet very large increase of the said participation in the whole region $\log \tau > -1$.

How an increase of the ratio $H:He$ influences an increase of the relative significance of ion-atom absorption processes with respect to the concurrent electron-atom process (3) in the mentioned spectral region is illustrated by Figs. 12 and 13 which show the behavior of the quantities $F_{e-He}^{(sim)}(\lambda; \log \tau)$ and $F_{e-He}^{(ia)}(\lambda; \log \tau)$ for $H:He = 10^{-4}$ and 10^{-3} respectively. From these figures one can see that for $H:He = \gtrsim 10^{-4}$ the inclusion of the non-symmetric processes (4) - (6) causes the ion-atom absorption processes to become absolutely domi-

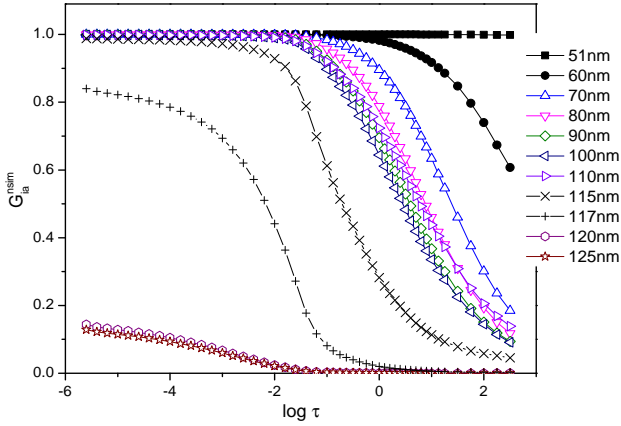


Figure 10. The behavior of the quantity $G_{ia}^{nsim} = \kappa_{nsim}/\kappa_{ia}$, see Eq. (17), for the atmosphere of a helium-rich white dwarf with $T_{eff}=12000$ K, $\log g = 8$ and $H/He=10^{-4}$.

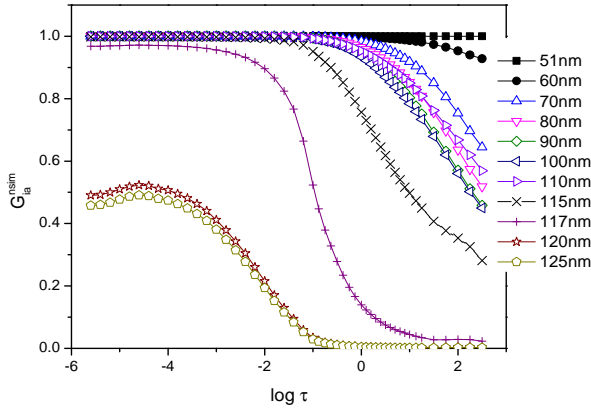


Figure 11. Same as in Fig. 10, but for $H:He=10^{-3}$.

nant with respect to the electron-atom process (3) in the greatest part of this region, namely for $51 \text{ nm} \leq \lambda \lesssim 110 \text{ nm}$, while for $\lambda > 110 \text{ nm}$ the efficiency of ion-atom processes stays close to the efficiency of the process (3).

In order to obtain the complete picture of the discussed absorption processes in the helium-rich white dwarf atmospheres in the cases $H:He=10^{-4}$ and 10^{-3} it is necessary again to include into the consideration the hydrogen photo-ionization process 7. The significance of partial absorption processes in such atmospheres within the whole region $\lambda > \lambda_{He}$ is illustrated in Fig's 14 and 15 where the corresponding plots of these processes are presented for $\log \tau = 0$. One can see that, as in the case of DB white dwarf, the process (7) in the region $\lambda_{He} < \lambda < \lambda_H$ gives the dominant contribution to the opacity of the considered atmospheres. Then, it has been established that in these cases this dominance also holds for any $\log \tau < 0$.

In accordance with our considerations, it is necessary to remind that the considered ion-atom absorption pro-

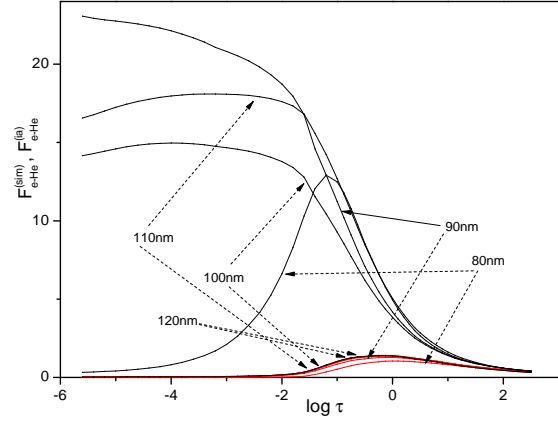


Figure 12. The behavior of the quantities $F_{e-He}^{(sim)}(\lambda; \log \tau) = \kappa_{sim}/\kappa_{ea}$ (red line i.e. lower line for the same λ) and $F_{e-He}^{(ia)}(\lambda; \log \tau) = \kappa_{ia}/\kappa_{ea}$ (black line i.e. upper line for the same λ), see Eq. (18), for the atmosphere of a helium rich white dwarf with $T_{eff}=12000$ K, $\log g = 8$ and $H/He=10^{-4}$.

cesses (symmetric and non-symmetric) can naturally be significant in the helium-rich white dwarf atmospheres with $T_{eff} < 20000\text{K}$, since at the higher temperatures electron ion absorption processes completely dominate with respect to the considered ion-atom and electron-atom processes. Therefore, it is necessary here to take into account the papers Bergeron et al. (2011) and Voss et al. (2007), where the data about numerous helium-rich white dwarfs are presented. Namely, from these one can see that the values $H:He$ which correspond to the helium-rich white dwarfs with $T_{eff} < 20000\text{K}$ are mainly situated between 10^{-5} and 10^{-4} , while the values $H:He > 10^{-4}$, especially $H:He$ close to 10^{-3} , have to be treated as certain extremes. But our results are supported by the following facts:

-firstly, from the results obtained it follows that the non-symmetric ion-atom processes cannot be neglected already for the case of atmospheres of DB white dwarfs with $H:He=10^{-5}$;

-secondly, from these results it follows that the effect of inclusion of the non-symmetric processes in the consideration fully manifests already for $H:He = 10^{-4}$, i.e. far from the extremum ($H:He=10^{-3}$, and remains practically the same further on. This makes important not just a neighborhood of the extremum value $H:He=10^{-3}$, but rather the whole region of $H:He > 10^{-5}$. Since from the presented results it follows that the ion-atom absorption processes should be especially significant in helium-rich white dwarf atmospheres with $H:He=10^{-4}$, this case is additionally illustrated by Fig. 16. In this figure the plots of the examined ion-atom absorption processes (symmetric and non-symmetric together) and of the referent electron-atom process (He^- -continuum) are presented for $\log \tau = -2, -1, -0.5, 0$ and 0.5 for the case $H:He=10^{-4}$. From Fig. 16 it can be clearly seen how the contribution of the non-symmetric ion-atom processes and the total efficiency of all the ion-atom processes with respect to the electron-atom processes changes with a change of $\log \tau$ in the whole region $\lambda > \lambda_{He}$.

At the end of this Section in Fig. 17 the behavior is illus-

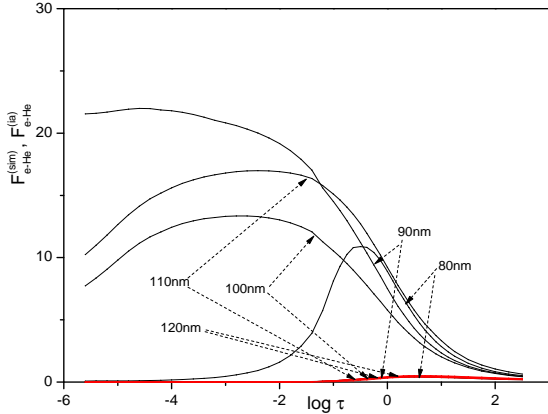


Figure 13. Same as in Fig. 12, but for $H:He=10^{-3}$.

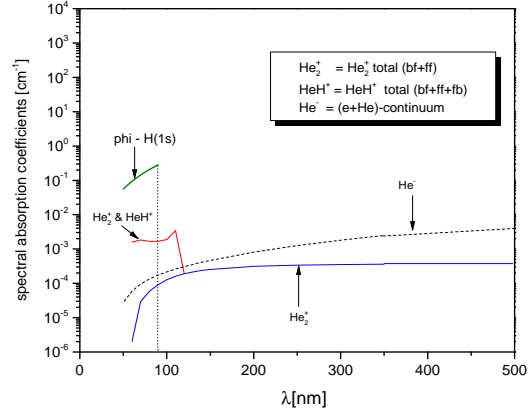


Figure 15. Same as in Fig. 14, but for $H:He=10^{-3}$.

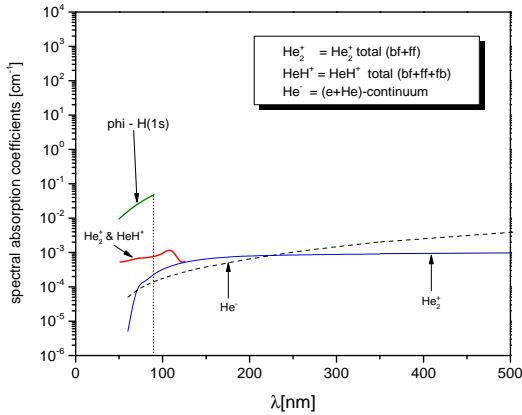


Figure 14. The plots of all considered absorption processes for $\log \tau = 0$ in the case of a helium-rich white dwarf with $T_{eff}=12000$ K, $\log g = 8$ and $H:He=10^{-4}$.

trated of the total ion-atom spectral absorption coefficient $\kappa_{ia}(\lambda; \log \tau)$, given by Eqs. (11), (13) and (16), for the considered examples of atmospheres of helium-rich white dwarfs with $T_{eff} = 12000$ K and $\log g = 8$: $H:He = 10^{-5}$, 10^{-4} and 10^{-3} . However, for the calculations of this absorption coefficient in the same approximation (existence of LTE), but for different atmospheres it is necessary to know the corresponding spectral rate coefficients, i.e. $K_{nsim}(\lambda, T)$, given by Eq. (12), and $K_{sim}(\lambda, T)$. Keeping in mind that the values of $K_{sim}(\lambda, T)$ can be determined by means of the data from Ignjatović et al. (2009), we calculated here only the values of the spectral rate coefficient $K_{nsim}(\lambda, T)$, within the corresponding regions of λ and T , which are presented in Table 1.

4 CONCLUSIONS

From the presented material it follows that the considered non-symmetric ion-atom absorption processes have to be

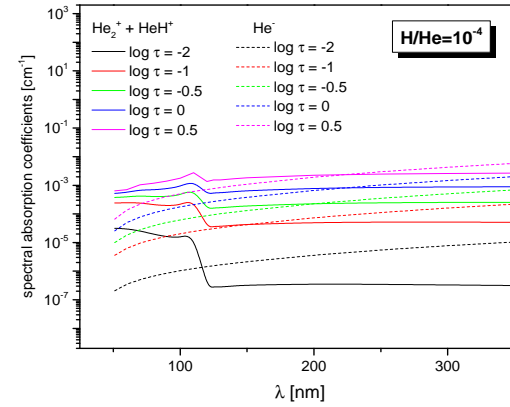


Figure 16. The plots of the examined ion-atom absorption processes (symmetric and non-symmetric together) and the referent electron-atom process (He^- -continuum) for $\log \tau = -2, -1, -0.5, 0$ and 0.5 in the case of a helium-rich white dwarf with $T_{eff}=12000$ K, $\log g = 8$ and $H:He=10^{-4}$.

treated as one of the important channels of influence on the opacity of the atmospheres of helium-rich white dwarfs in the far UV and EUV region. So, it has been shown that even in the case of DB white dwarfs with $H:He = 10^{-5}$ such processes should be included in the models of their atmospheres. However, the main result of this research is the establishment of the fact that in the cases of helium-rich white dwarfs with $H:He > 10^{-5}$, and particularly with $H:He = 10^{-4}$, these non-symmetric ion-atom absorption processes have to be included *ab initio* in the models of the corresponding atmospheres, since in the greater part of the considered far UV and EUV region they could be completely dominant with respect to the referent electron-atom and symmetric ion-atom absorption processes.

Besides, attention has been paid again in this paper to the role of the hydrogen component in the atmospheres of helium-rich white dwarfs. Namely, it has been shown that in all the considered cases ($H:He = 10^{-5}, 10^{-4}$ and 10^{-3})

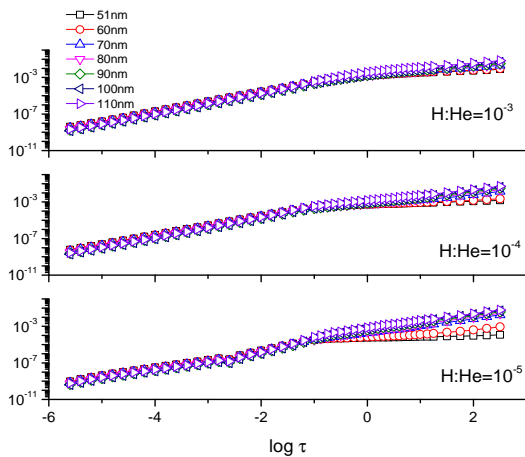


Figure 17. The behavior of the total ion-atom spectral absorption coefficient $\kappa_{ia}(\lambda; \log \tau)$, see Eqs. (11), (13) and (16), in the cases of the atmospheres of helium rich white dwarfs with $T_{eff} = 12000$ K and $\log g = 8$ for: H:He = 10^{-5} , H:He = 10^{-4} and H:He = 10^{-3} .

the hydrogen photo-ionization processes (7) yield a dominant contribution to the opacity of the corresponding atmospheres in the region $\lambda_{He} < \lambda < \lambda_H$.

As a task for further investigations in this area the study can be mentioned of the atmospheres of helium-rich white dwarfs with smaller effective temperatures (≈ 7000 K) where the significance of the hydrogen component can be greater than in the described cases. Also, inclusion into consideration would be useful of the ion-atom non-symmetric absorption processes with participation of some metal components of the considered atmospheres.

ACKNOWLEDGMENTS

The authors are very grateful to Prof. D. Koester for providing the data of helium-rich white dwarfs atmosphere models and to Prof. P. Bergeron for a very wide and fruitful discussion. Also, the authors are thankful to the Ministry of Education, Science and Technological Development of the Republic of Serbia for the support of this work within the projects 176002 and III4402.

REFERENCES

- Bergeron, P., Wesemael, F., & Beauchamp, A. 1995, *PASP*, 107, 1047
 Bergeron, P., Wesemael, F., Dufour, P., et al. 2011, *ApJ*, 737, 28
 Bergeron, P. 2013, private communication
 Bethe, H. A., & Salpeter, E. E. 1957, *Quantum Mechanics of One- and Two-Electron Atoms*, New York: Academic Press, 1957,
 Bues, I. 1970, *A&A*, 7, 91
 Dufour, P., Bergeron, P., Schmidt, G. D., Liebert, J., Harris, H. C., Knapp, G. R., Anderson, S. F., & Schneider, D. P. 2006, *ApJ*, 651, 1112

- Dufour, P., Bergeron, P., Liebert, J., Harris, H. C., Knapp, G. R., Anderson, S. F., Hall, P. B., Strauss, M. A., Collinge, M. J., & Edwards, M. C. 2007, *ApJ*, 663, 1291
 Dumitriu, I., & Saenz, A. 2009, *Journal of Physics B Atomic Molecular Physics*, 42, 165101
 Fontenla, J. M., Curdt, W., Haberreiter, M., Harder, J., & Tian, H. 2009, *ApJ*, 707, 482
 Green, T. A., Browne, J. C., Michels, H. H., & Madsen, M. M. 1974a, *J. Chem. Phys.*, 61, 5198
 Green, T. A., Michels, H. H., Browne, J. C., & Madsen, M. M. 1974b, *J. Chem. Phys.*, 61, 5186
 Ignjatović, L. M., Mihajlov, A. A., Sakan, N. M., Dimitrijević, M. S., & Metropoulos, A. 2009, *MNRAS*, 396, 2201
 Koester, D. 1980, *A&AS*, 39, 401
 Koester, D. 2010, *Mem. Soc. Astron. Italiana*, 81, 921
 Koester, D. 2013, private communication
 Mihajlov, A. A., & Dimitrijević, M. S. 1986, *A&A*, 155, 319
 Mihajlov, A. A., & Dimitrijević, M. S. 1992, *A&A*, 256, 305
 Mihajlov, A. A., Dimitrijević, M. S., & Ignjatović, L. M. 1993, *A&A*, 276, 187
 Mihajlov, A., Dimitrijević, M., & Ignjatović, L. 1994a, *A&A*, 287, 1026
 Mihajlov, A. A., Dimitrijević, M. S., Ignjatović, L. M., & Djurić, Z. 1994b, *A&AS*, 103, 57
 Mihajlov, A. A., Dimitrijević, M. S., Ignjatović, L. M., & Djurić, Z. 1995, *ApJ*, 454, 420
 Mihajlov, A. A., Ignjatović, L. M., Sakan, N. M., & Dimitrijević, M. S. 2007, *A&A*, 437, 1023
 Mihajlov, A. A., Ignjatović, L. M., Srećković, V. A., Dimitrijević, M. S., & Metropoulos, A. 2013, *MNRAS*, 431, 589
 Somerville, W. B. 1965, *ApJ*, 141, 811
 Stancil, P. C. 1994, *ApJ*, 430, 360
 Voss, B., Koester, D., Napiwotzki, R., Christlieb, N., & Reimers, D. 2007, *A&A*, 470, 1079
 Wegner, G., & Koester, D. 1985, *ApJ*, 288, 746

Table 1. The spectral absorption rate coefficient $K_{nsim}(\lambda; T)$, see Eq. (12), calculated under the condition of existence of local thermodynamic equilibrium.

λ [nm]	T [10^3K]						
	8	10	12	14	16	18	20
51	3.24E-40	1.68E-40	1.04E-40	7.22E-41	5.37E-41	4.19E-41	3.39E-41
55	3.36E-40	1.83E-40	1.19E-40	8.58E-41	6.66E-41	5.43E-41	4.58E-41
60	3.19E-40	1.85E-40	1.26E-40	9.54E-41	7.70E-41	6.51E-41	5.68E-41
65	2.89E-40	1.78E-40	1.28E-40	1.01E-40	8.39E-41	7.29E-41	6.52E-41
70	2.65E-40	1.75E-40	1.33E-40	1.09E-40	9.36E-41	8.31E-41	7.54E-41
75	2.33E-40	1.61E-40	1.26E-40	1.06E-40	9.31E-41	8.38E-41	7.68E-41
80	2.09E-40	1.53E-40	1.24E-40	1.07E-40	9.61E-41	8.80E-41	8.20E-41
85	1.93E-40	1.48E-40	1.25E-40	1.11E-40	1.02E-40	9.48E-41	8.94E-41
90	1.84E-40	1.49E-40	1.30E-40	1.19E-40	1.11E-40	1.05E-40	1.00E-40
95	1.83E-40	1.56E-40	1.41E-40	1.32E-40	1.25E-40	1.20E-40	1.16E-40
100	1.91E-40	1.73E-40	1.61E-40	1.53E-40	1.47E-40	1.43E-40	1.40E-40
105	2.24E-40	2.16E-40	2.05E-40	1.97E-40	1.92E-40	1.90E-40	1.89E-40
110	3.38E-40	3.10E-40	3.07E-40	3.06E-40	3.04E-40	3.03E-40	3.02E-40
115	5.53E-41	6.74E-41	7.70E-41	8.65E-41	9.49E-41	1.02E-40	1.10E-40
120	3.14E-42	2.75E-42	2.62E-42	2.48E-42	2.25E-42	1.93E-42	1.62E-42
125	3.11E-42	2.58E-42	2.51E-42	2.45E-42	2.19E-42	1.75E-42	1.31E-42